DESIGNING FRAMEWORK OF A SEGMENTED RUBBER TRACKED VEHICLE FOR SEPANG PEAT TERRAIN IN MALAYSIA

ATAUR RAHMAN*, AZMI YAHAYA, MOHD. ZOHADIE, DESA AHMAD AND WAN ISHAK

Faculty of Engineering, University Putra Malaysia,

43400,Serdang, Selangor,Darul Ehsan, Malaysia

Abstract: The focus of this paper to present the designing framework of an off-road special segmented rubber tracked vehicle that may be required to run on low bearing capacity peat terrain. To complete this study: *firstly*, mechanical properties of peat terrain were first determined by using different type of apparatus. Direct shear test was performed using a Wykeham Farrance 25402 shear box apparatus to determine the internal friction angle, cohesiveness and shear deformation modulus of the peat sample. Load-sinkage test was performed using a specially made bearing capacity apparatus to determine the stiffness values of surface mat and underlying peat. *Secondly*, substantiate the validity of the mathematical model and *finally* design parameters of the special segmented rubber tracked vehicle were optimized by simulation.

Keywords: *Tracked vehicle, peat terrain, tractive performance.*

1. INTRODUCTION

In Malaysia, new requirements for greater mobility over a wide range of peat terrain, and growing demands for environmental protection and collection-transportation goods by vehicles on unprepared peat terrain constitute a significant part of the overall transportation activities. This has led to the necessity of developing segmented rubber tracked vehicle and establishing mathematical models for the vehicle-peat terrain systems, that will enable design engineers, as well as users, to evaluate a wide range of options for the selection of an optimum configuration for a given mission and environment. Various organizations in Malaysia are introduced different type of machines for performing several tasks on peat land. The machines suitabilities were justified based on the mechanical properties [2] of Sepang peat land. It was found that the engine power of all the machines are quite reasonable based on their carrying capacity. However, the tractive performances is severely effected due to the higher ground pressure distribution.

* Corresponding author

2. MATERIALS AND METHODS

The feasibility of the land locomotion of the tracked vehicle operating on the weak peat terrain is discussed from the perspective of the terramechanics. Figure 1 shows the processes for designing a segmented tracked vehicle. This paper presents the discussion until the design parameter optimization technique.

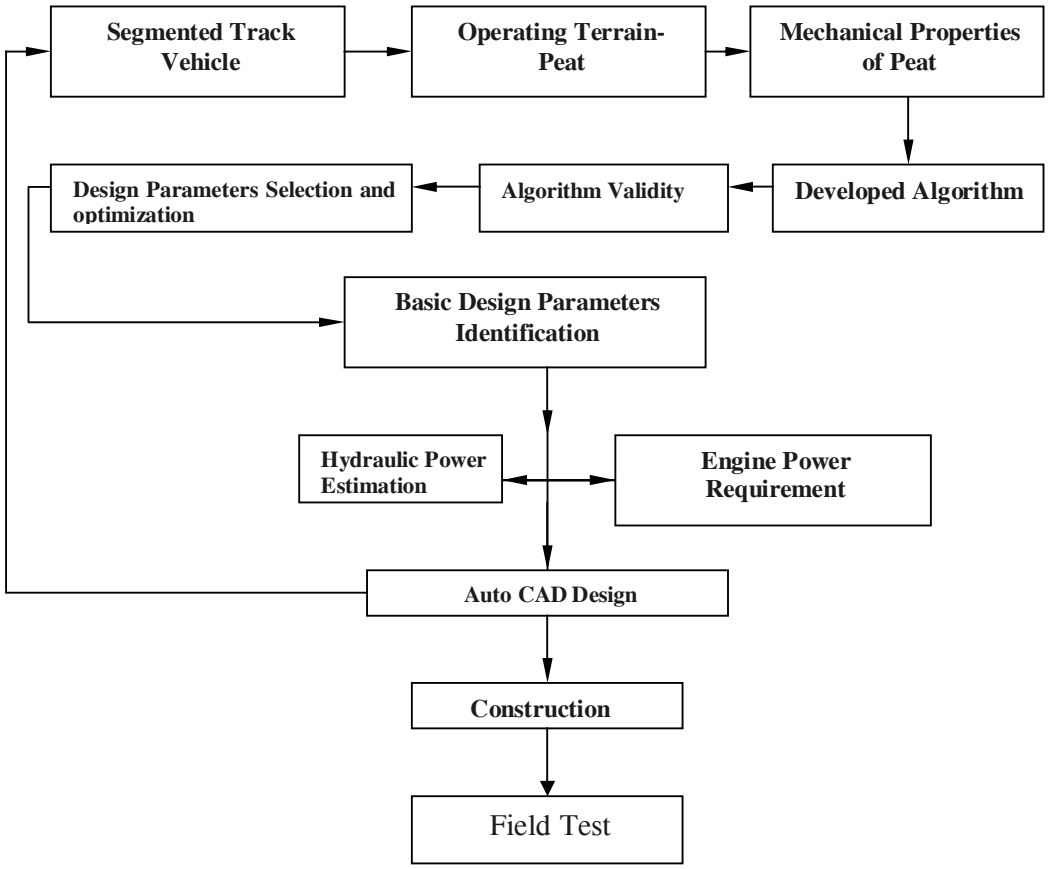

Fig. 1: Flow chart for the processes of designing a segmented tracked vehicle.

2.1 Mechanical Properties of Peat Terrain

To properly identify the mechanical properties of peat from a vehicle mobility viewpoint, measurement has been taken under loading conditions similar to those exerted by a vehicle on the peat terrain. Field tests were carried out at Sepang peat area, located about 45 km from Kuala Lumpur Malaysia for determining the mechanical properties of peat terrain including moisture content, bulk density, cohesiveness, internal friction angle, shear deformation modulus, vane shearing strength, surface mat stiffness, and underlying stiffness of peat. The mechanical properties of Sepang peat terrain including the terrain moisture content ω, bulk density γ_d, peat surface mat stiffness m_m, underlying stiffness of peat k_p, cohesiveness c, internal frictional angle φ, and shear deformation modulus K_w that are found from an earlier work [2] are given in Table 1.

Table 1. Peat terrain parameters.

Parameters	Un-drained		Drained	
	Mean value	SD	Mean value	SD
ω, (%)	83.51	-	79.58	-
γ_d, (kN/m^3)	1.53	0.59	1.82	0.78
c, kN/m^2)	1.36	0.21	2.73	0.39
φ, (degree)	23.78	4.56	27.22	2.19
K_w, (cm)	1.19	0.10	1.12	0.17
m_m,(kN/m^3)	27.07	13.47	41.79	13.37
k_p, (kN/m^3)	224.38	52.84	356.8	74.27

Notification: SD-Standard deviation, Source: [2].

2.2 Mathematical Model

Consider a rigid link segmented rubber track vehicle of weight W, track size including track ground contact length *L*, width *B*, pitch T_p, and grouser height *H*, radius of the front idler R_{fi} , rear sprocket R_{rs}, and road-wheel R_w, and height of center of gravity (C.G) h_{cg}, which is traversing under traction on a peat terrain at a constant speed of v_t and applied a driving torque *Q* at the rear sprocket by the hydraulic motor as in Fig. 10. If the pressure distribution in the track-terrain interface is assumed to be non-uniform by locating vehicle C.G rearward of the track mid point, the vehicle will traverse on the specified terrain by making an angle θ_{ti}. Consequently, the track entry and exit angles at the front idler θ_{fi} and rear sprocket θ_{rs}, the reaction pressure at the front idler P_{fi}, main straight part P_o, and rear sprocket P_{rs}, and the sinkage of the front idler z_{fi}, main straight part z_{mp}, and rear sprocket z_{rs} and tangential force reveal different values due to the different amount of slippage at each of the grouser positions of the rigid link tracks at the bottom track elements of the front idler i_{fi}, main straight parts i_{mp} , and rear sprocket i_{rs} as shown in Fig. 2.

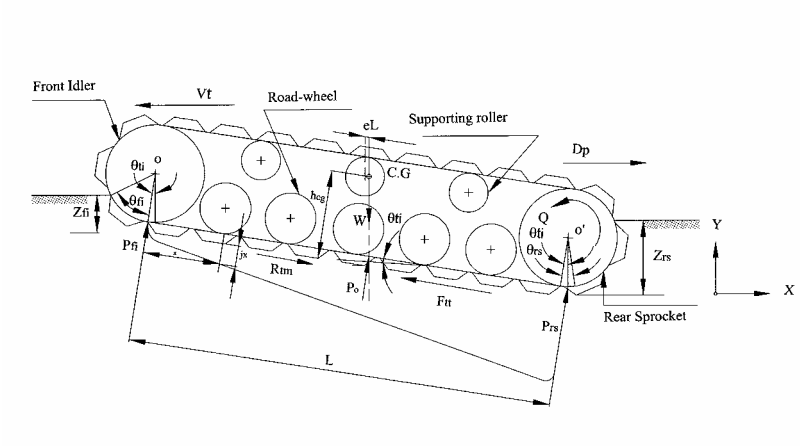

Fig. 2: Force acting on the track system of the vehicle during traversing on peat terrain with a slippage of 10%.

The following assumptions were made in order for the equation used in the mathematical modelling to be valided:

i. Vehicle theoretical speed was considered to be 10 km/hr on zero slope terrain based on various off-road operations ASAE D497.3 NOV96, ASAE standard (1996).
ii. Vehicle total weight was considered to be 19.62 kN with payload of 9.81kN based on the in-field maximum fresh bunches collection practiced.
iii. Vehicle's track critical sinkage was considered to be 0.1m based on experimental data on Sepang Peat terrain [2].
iv. Aerodynamic resistance was neglected, due to the low operating speed.
v. Vehicle's belly drag was considered to be zero since the vehicle hull was not in contact with the terrain.
vi. Vehicle speed fluctuation was considered to be 2.75% based on Wong [7].
vii. Road-wheel spacing was considered to be 0.245m to ensure good drawbar performance based on Wong [7].

2.2.1 Slippage

Slippage is one of the functional parameters for the vehicle traction mechanism. It reveals different value at the bottom track part of front idler, main straight part, and rear sprocket if the vehicle traverses on unprepared peat terrain with non-uniform ground pressure distribution. Therefore, it is important to compute the slippage of the front idler, track main straight part, and rear sprocket separately to determine the vehicle performance over the peat terrain.

For the slippage of the ground contact track of front idler, the relationship between the front idler slippage i_{fi} , the entry angle of the track at front idler θ_{fi} , the track trim angle θ_{ti}, the slippage ratio i and front idler radius R_{fi} can be modeled by the following equation [5].

$$i_{fi} = \left(\frac{R_{fi}}{L_{fi}} \right)_{fi} \left[\theta_{fi} - (1-i) \left\{ \sin\left(\theta_{fi} + \theta_{ti}\right) - \sin\theta_{ti} \right\} \right] \tag{1}$$

where, the slip ratio, $i = \frac{v_t - v_a}{v_t}$, track trim angle, $\theta_{ti} = \arcsin\left(\left(z_{rs} - z_{fi} \right) / L \right)$, and track entry angle $\theta_{fi} = \arccos\left(\cos\theta_{ti} - z_{fi} / R_{fi} \right)$ and $L_{fi} = R_{fi}\left(\theta_{fi} + \theta_{ti}\right)$.

For the slippage of the ground contact track of rear sprocket, the relationship between the slippage of rear sprocket i_{rs} and front idler i_{fi}, rear sprocket radius R_{rs}, the track entry

angle θ_{fi}, the track trim angle θ_{ti}, and exit angle θ_{rs} can be modeled by the following equation of Ataur *et al.*[5] :

$$i_{rs} = i_{fi} + i\left(\frac{L_{rs}}{L}\right) + \left(\frac{R_{rs}}{L_{rs}}\right)\left[\theta_{rs} + (1-i)\sin(\theta_{rs} + \theta_{ti}) - \sin\theta_{ti}\right] \quad (2)$$

where, track exit angle $\theta_{rs} = \arcsin\left(\frac{z_{rs} - z_{fi}}{L}\right) + \arccos\left[\frac{R_{rs}}{\sqrt{\left\{R_{rs}^{\,2} - \left(z_{rs}^{\,2} - z_{fi}^{\,2}\right)\right\}^2}}\right]$, sinkage of the front idler, $z_{fi} = \frac{-\left(\frac{k_p D_{hfi}}{4m_m}\right) \pm \sqrt{\left[\left(\frac{k_p D_{hfi}}{4m_m}\right)^2 + \frac{D_{hfi}\, p_{fi}}{m_m}\right]}}{2}$, sinkage of the rear sprocket, $z_{rs} = \frac{-\left(\frac{k_p D_{hrs}}{4m_m}\right) \pm \sqrt{\left[\left(\frac{k_p D_{hrs}}{4m_m}\right)^2 + \frac{D_{hrs}\, p_{rs}}{m_m}\right]}}{2}$, hydraulic diameter of the terrain due to front idler, $D_{hfi} = \frac{4BL_{fib}}{2(L_{fib} + B)}$, rear sprocket, $D_{hfi} = \frac{4BL_{rsb}}{2(L_{rsb} + B)}$ and $L_{rs} = R_{rs}(\theta_{rs} + \theta_{ti})$.

2.2.2 Tractive Effort

The tractive effort is denveloped not only on the ground contact part of the track but also on the side parts of the ground contact track grouser and on parts of front idler and rear sprocket. The initial track tension 12% of the total vehicle weight is assumed to be constant in every point of the track system in order to avoid the track deflection apparently between consecutive road-wheels.

2.3 Ground Contact Part of the Track

The traction mechanics of the track bottom part of the front idler, road-wheels, and rear sprocket are different due to its different angle of entry and exit. It is also different due to the different sinkage of the track front idler, main straight part, and rear sprocket when the vehicle traverses on the unprepared peat terrain with non-uniform ground pressure distribution. Therefore, it is important to compute the traction of the individual components bottom track segment, separately.

For the tractive effort developed at the track ground contact length of the front idler, the relationship between the tractive effort F_b developed at the ground contact track, track ground contact length L, track width B, terrain cohesiveness c, normal stress σ, shear stress τ, shear deformation modulus K_w, and slippage ratio of the track-terrain interfaces i can be modeled by the following equation of Ataur *et al.*[5]:

$$F_{fib} = 2BL_{fib}\left(c + \sigma\tan\varphi\right)\left[\frac{e^{1}K_{wfi}}{i_{fi}L_{fib}} - \left(1 + \frac{K_{wfi}}{i_{fi}L_{fib}}\right)\exp\left(1 - \frac{i_{fi}L_{fib}}{K_{wfi}}\right)\right] \quad (3)$$

with $L_{fib} = R_{fi}\left(\theta_{fi} + \theta_{ti}\right)$

The tractive effort of the track main straight part and rear sprocket ground contact track was computed by Eq. (3).

2.4 Side of the Ground Contact Track

Wong [7] suggested that the traction mechanics of the track at the side of the grouser is highly significant on the development of vehicle traction if the vehicle sinkage is more than the grouser height. In this study, it was assumed that the sinkage of the vehicle was more than the grouser height of the vehicles track.

For the tractive effort developed at the side of the ground contact length of the front idler track, the relationship between the tractive effort F_s developed at the side of the track ground contact part, track grouser height H, track ground contact length L, terrain cohesiveness c, normal stress σ, shear stress τ, shear deformation modulus K_w, and slippage i of the vehicle track-terrain interfaces can be modeled by the following equation of Ataur *et al*. [5]:

$$F_{fis} = 4HL_{fib}\left(c + \sigma \tan\varphi\right)\cos\alpha\left[\frac{e^1 K_{wfi}}{i_{fi}L_{fib}} - \left(1 + \frac{K_{wfi}}{i_{fi}L_{fib}}\right)\exp\left(1 - \frac{i_{fi}L_{fib}}{K_{wfi}}\right)\right] \tag{4}$$

with $\alpha = \arctan\left[\cot\left(\frac{H}{B}\right)\right]$

The tractive effort at the side of the track main straight part and rear sprocket ground contact track was computed using Eq. (4).

2.5 MOTION RESISTANCE

When the same vehicle as shown in Fig. 2, traverses on the peat terrain with non-uniform pressure distribution, the vehicle individual components such as front idler, main straight part, and rear sprocket reveal different values of motion resistances due to the different sinkages. Therefore, it is important to compute the motion resistance of the individual component for understanding the vehicle performance.

For the motion resistance of the vehicle due to terrain compaction R_c, the ground contact length L, track width B, sinkage of the vehicle z, stiffness of peat surface mat m_m and underlying peat k_p can be modeled by equation of Ataur *et al*. [5]:

$$R_c = (2B)\left[\begin{array}{l}\left(\frac{L_{fi}}{L}\right)\left(\frac{k_p z_{fi}^{\ 2}}{2} + \frac{4}{3D_{hfi}} m_m z_{fi}^{\ 3}\right) + \left(\frac{L_{mp}}{L}\right)\left(\frac{k_p z_{mp}^{\ 2}}{2} + \frac{4}{3D_{hmp}} m_m z_{mp}^{\ 3}\right) \\ + \left(\frac{L_{rs}}{L}\right)\left(\frac{k_p z_{rs}^{\ 2}}{2} + \frac{4}{3D_{hrs}} m_m z_{rs}^{\ 3}\right)\end{array}\right] \tag{5}$$

where

$$D_{hfi} = \frac{4BL_{fi}}{2(L_{fi} + B)},\ D_{hmp} = \frac{4BL_{mp}}{2(L_{mp} + B)},\ \text{and}\ D_{hrs} = \frac{4BL_{rs}}{2(L_{rs} + B)}$$

For the motion resistance of the vehicle due to bull dozing effect, the relationship between the motion resistance of the vehicle due to bull dozing effect R_b, the bulk density of the terrain γ_d, the internal frictional angle φ, track width B, and terrain cohesiveness c can be modeled by the following general equation of Wong [7]:

$$R_b = 2B\left[\gamma_d z^2 \tan^2\left(45 + \frac{\varphi}{2}\right) + cz \tan\left(45 + \frac{\varphi}{2}\right)\right] \quad (6)$$

The total external motion resistance of the rubber track vehicle R_{tm}, can be computed as the sum of the individual motion resistance components by:

$$R_{etm} = R_{fic} + R_{msc} + R_{rsc} + R_{fib} + R_{msb} + R_{rsb} \quad (7)$$

2.6 Sprocket Torque

When torque is applied at the sprocket, it starts driving the track and the vehicle starts moving. A frictional torque appears in the bearings of moving elements of the track system, resisting the vehicle motion. The forces appear at the track interface due to the terrain compaction and vehicle bulldozing effect, resisting the vehicle motion. Therefore, the vehicle needs to develop sufficient tractive effort after developing shear stress at the track-terrain interface in order to move forward and overcoming all of the motion resistance. The tension in each track segment does not affect the torque of the vehicle motion since it was assumed to be constant due to the geometrical arrangement of the road-wheel and initial tension equals to 12% of the total weight of the vehicle. For the torque of the sprocket, the relationship between the torque of the sprocket Q, vehicle total tractive effort F_{tt}, total motion resistance $R_{tm,}$ sprocket radius R_{rs}, track grouser height H, vehicle total weight W, and vehicle normal reaction force F_n and track ground contact length L can be modeled by using the following equation:

$$Q = D_p(R_{rs} + H) + W(h_{cg} - R_{rs})\sin\theta_{ti} + L(F_n - W)(0.5 - e)\cos\theta_{ti} \quad (8)$$

where

$$F_n = \frac{W - F_{tt}\sin\theta_{ti}}{\cos\theta_{ti}}$$

2.7 Vehicle Steerability

The force system assumed to be acting on a tracked vehicle in general planar motion is shown in Fig. 3 and Fig. 4. In these figures, F_{ot} and F_{it} are the thrusts on the outer and inner tracks. R_{lnot} and R_{lnit} are the longitudinal forces exerted by the terrain to per unit length of the outer and inner track, f_r and μ_l are the coefficients of the longitudinal and lateral motion resistance, respectively, B_{stc} is the vehicle tracks tread, F_{cent} is the centrifugal force and β is the slip angle. Kitano and Kuma (1977) and Shiller et al. (1993) stated that the slip angle β appears to zero during the straight line motion, and has some signed value when the vehicle turns left or right.

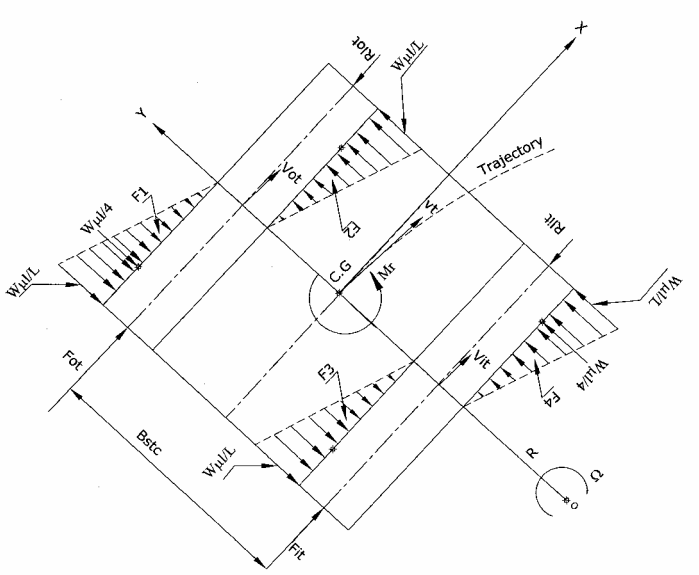

Fig. 3: Force acting on the track during turning at 6 km/hr.

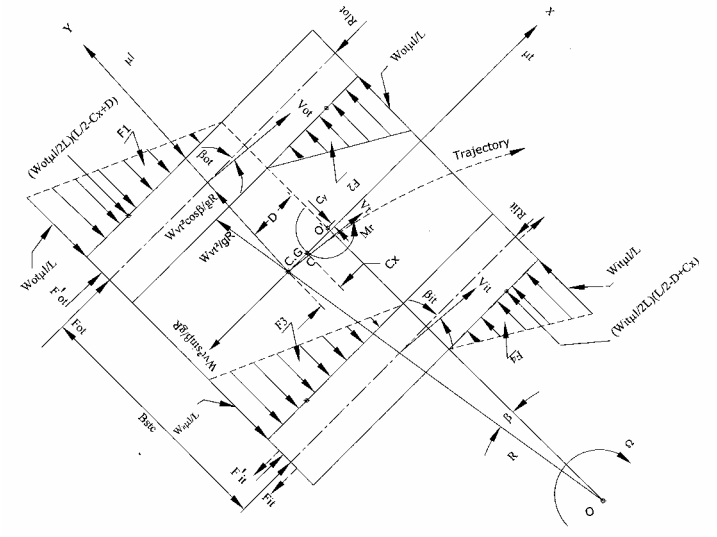

Fig. 4. Force acting on the track during turning at 10 km/hr.

During a turn, centrifugal force appears at the mass centre of the vehicle. When the vehicle turns at a traveling speed of 6 km/hr with locating C.G at the middle of the track system, the slip angle of the vehicle is assumed to be zero due to negligible effect of centrifugal forces. The lateral motion resistance assumed to be equally distributed around the C.G of the vehicle and represented by equal triangles *F*1 to *F*4 as shown in Fig. 3. When the vehicle turns at a traveling speed of 10km/hr with locating C.G at 0.20 m rearward from the middle point of the track system, the slip angle of the track system β is considered significant higher value and significantly affect the vehicle stability and steerability. Therefore, the lateral force distributions on the track system to be congruent are represented by the triangles F1 to F4 as shown in Fig. 4. The vehicle must have rotated about an instantaneous center point O′ located at a distance of D ahead of the vehicle C.G for the dynamic equilibrium. This force is generated by a shift to the point O′ ahead of *C.G* and the vehicle will be oriented by an slip angle β, which can be computed as $\beta = \arctan\left(\Omega^2 L / 4g\mu_l\right)$, the yaw velocity Ω of the vehicle can be computed as $\Omega = (R_{rs})\left(\frac{\omega_{ot} + \omega_{it}}{2R}\right)$,where, R_{rs} is the radius of the sprocket. The vehicle follows the dashed trajectory, turning to the right around the instantaneous centre point O′ with turning radius *R*.

2.8 Dynamic load on the Tracks

From the slippage equations of the outer and the inner track it can be identified that when the loading condition of the vehicle changes, as the vehicle is accelerating, the slippages of the vehicle track changes. Therefore, in order to adjust the vehicle slippage on given terrain it is necessary to estimate the proper loading condition for getting the high steerability of the vehicle The centrifugal force of the vehicle that will develop during turning at speed of 10km/hr can be computed as $F_{cent} = W\Omega^2 R\cos\beta / g$, which causes lateral load transfer. The weight transfer from the inner track to the outer track is mainly due to the centrifugal force. If the centrifugal force is taken into consideration the dynamic loads of the outside and inside track will be different. For the dynamic load of the vehicle outer and inner track, the relationship between the dynamic load of outside and inside track W_{ot} and W_{it}, yaw movement of the vehicle Ω, turning radius *R,* slip angle β and acceleration due to gravity *g,* can be modeled using the following equations of Ataur *et al.*[3]:

$$W_{ot} = \frac{W}{2} + \frac{h_{cg} W\Omega^2 R}{B_{stc} g}\cos\beta \tag{9}$$

$$W_{it} = \frac{W}{2} - \frac{h_{cg} W\Omega^2 R}{B_{stc} g}\cos\beta \tag{10}$$

where $\beta = \arctan\left(\frac{D}{R}\right)$

Drawbar pull

The drawbar power is referred to as the potential productivity of the vehicle, that is, the rate at which productive work may be done. It is computed using the following equation:

$$P_d = D_p V_a \tag{11}$$

with $D_p = F_{tt} - R_{tm}$

Tractive efficiency

Tractive efficiency is used to characterize the efficiency of the track vehicle in transforming the engine power to the power available at the drawbar. It is defined by the following equation:

$$\eta_d = \frac{P_d}{P_e} \tag{12}$$

3. MATHEMATICAL MODEL VALIDATION

The drawbar pull and the tractive efficiency of light peat prototype Kubota Carrier RC20P track vehicle having track width of 0.43 m, track ground contact length of 1.85 m, total weight of 2645 kg including payload 1000 kg and three pneumatic road-wheels on each track, operating on a peat terrain were predicted through simulation. Basic parameters of the reference vehicle that used in the study are shown in Table 2.

Table 2. Basic parameters of Kubota Carrier RC20P track vehicle.

Parameters	Symbol	Values
Vehicle parameters		
Machine weight, kN	W	1645
Max. loading capacity, kN	W_l	1000
Rated power, kW@rpm	P	8.2@3200
Track parameters		
Ground contact length, m	L	1.85
Width, m	B	0.43
Grouser height, m	H	0.05
Machine parameters		
Length, m	L_t	2.98
Width, m	B_t	1.76
Height, m	H_t	1.45
Ground clearance, m	G_c	0.27

Source: Ooi [6]

Table 3 shows that the regression model is highly significant at a significance level of $P_r<0.01$. In the regression model, t values of 11.74 for i and –7.84 for i^2 are higher than t^*_{16} (0.01)=2.69. Hence, the null hypothesis is rejected. This implies that the slippage of the vehicle has significant effect on the drawbar pull of the vehicle. A standard error value of 0.032 for i and 0.00067 for i^2 are concluded that both of the predicted and measured drawbar pull is pretty tightly bunched together. The variability of the predicted and measured drawbar pulls of the vehicle has the less variability around the best fitted regression line, $D_p = 0.916 + 0.385(i) - 0.005(i^2)$ where, D_p is the drawbar pull of the vehicle in kN and i is the slippage of the vehicle in percentage. Therefore, based on the vehicle estimated standard error of 0.032 and the R-square values of 0.967, it can be concluded that the predicted and the measured drawbar pull are strongly correlated.

Table 3: Regression analysis on the drawbar pull of Kubota Carrier RC20P track vehicle.

Source	df	SS	F value	P value	R square
Model	2	99.97650	49.98825	0.0001	0.9667
Error	16	4.52226	0.28264		
C total	18	104.49876			

Estimated Parameter	Coefficient	T for H0: Parameter=0	Standard Error	P_r <[T]
Intercept	0.916190	3.431	0.26699892	0.0034
i	0.385447	11.794	0.03268138	0.0001
i^2	-0.005228	-7.842	0.00066673	0.0001

Table 4 shows that the slippage of the vehicle significantly (P_r <0.01) affects the vehicle drawbar pull. While, the non-significant value of treatments (predicted and measured drawbar pull) indicates that there is no significant difference between the treatments. Therefore, the close agreement between the predicted and measured drawbar pull of the vehicle substantiates the validity of the simulation model.

Table 4: ANOVA on the drawbar pull of Kubota Carrier RC20P track vehicle

Slippage	18	201.47489383	143.21	0.0001
Treatment	1	0.14455325	1.85	0.1906
Error	18	1.40688027		
Total	37	203.02632735		

Table 5 shows that the regression model is highly significant at significance level of $P_r<0.01$. In the regression model, t values of 2.91 for i and -3.81 for i^2 are higher than $t^*_{35}(0.01) = 2.67$. Hence, the null hypothesis is rejected. This implies that the slippage of the vehicle has significant effect on the tractive efficiency of the vehicle. The standard error values of 0.23 for i and 0.0087 for i^2 concluded that both of the predicted and measured drawbar pull are pretty tightly bunched together. The variability of the predicted

and measured drawbar pulls of the vehicle have less variability around the best fitted regression line, $T = 56.61 + 1.25(i) - 0.0034(i^2)$ where, T is the tractive efficiency of the vehicle in percentage and i is the slippage of the vehicle in percentage. Therefore, based on the standard error estimated values of the vehicle of 0.23 and the R-square value of 0.79, it can be concluded that the predicted and the measured drawbar pulls are strongly correlated.

Table 5: Regression analysis on the tractive efficiency of Kubota Carrier RC20P track .vehicle

Source	df	SS	F value	P	
Model	2	2604.69	13.31	0.0001	0.793
Error	35	3426.12			
C total	37	6030			
Estimated	Coefficient	T for H0:	Standard	P_r<[T]	
Intercept	56.61	15.83	3.51	0.0001	

Table 6 shows that the slippage of the vehicle significantly (P_r <0.01) affects the tractive efficiency of the vehicle. The non-significant value of treatments (predicted and measured tractive efficiency) indicates that there is no significant difference between the treatments on the model. Therefore, the closed agreement between the predicted and measured tractive efficiency of the vehicle substantiates the validity of the simulation model.

Table 6: ANOVA on the tractive efficiency of Kubota Carrier RC20P track vehicle.

Source	df	SS	F value	P value
Slippage	18	6153.59	2556.23	0.0001
Treatment	1	0.006	0.05	0.83
Error	18	2.28		
Total	37	203.026		

4. VEHICLE DESIGN PARAMETERS OPTIMIZATION

Tractive performance of the rigid link segmented rubber tracked vehicle has been computed with the computer simulation method based on the new mathematical model for undrained peat terrain. It appeared that the engine size and tractive performance of the vehicle on peat terrain vary with: the variation of vehicle weight, track size including track ground contact length, width, pitch and grouser height track entry and exit angle, idler diameter and location, sprocket diameter and location, road-wheel diameter, spacing and geometrical arrangement, and location of center of gravity. Therefore, for the selection and optimization design parameters of the vehicle track size, idler diameter and location,

sprocket diameter and location, number of road-wheel, road-wheel diameter, spacing and geometrical arrangement, ratio of the road wheel spacing to track pitch, ratio of the sprocket diameter to track pitch, and the location of the center of gravity are taken into account. The optimization design parameters of the vehicle have been performed by using the Microsoft Excel software with performing calculations, analyzing information and managing lists in spreadsheets.

4.1 Track Width and Ground Contact Length

The length of the track in contact with the ground and the level of pressure within the ground are the most important factors that influenced tracked vehicle tractive performance. To evaluate the effects of track system configuration on the vehicle ground pressure distribution and surface mat stiffness, it is important to study track ground contact length and width. Figures 5(a) and 5(b) show that the vehicle ground pressure distribution decreases with increasing vehicle track ground contact length and width. The vehicles under consideration are traversing on a zero slope terrain with a travel speed of 10 km/hr. From the field experiment on Sepang, it was found that the bearing capacity for the un-drained peat terrain was 17 kN/m^2. It appears that if a ground contact pressure of the 19.62 kN vehicle, with a moderate payload of 5.89 kN, is limited to 16.35 kN/m^2 by designing a track with ground contact area of 30x2000 mm^2 then the sinkage and external motion resistance of the vehicle will be low and tractive effort will be high, yielding a desired travel speed of 10 km/hr and vehicle productivity.

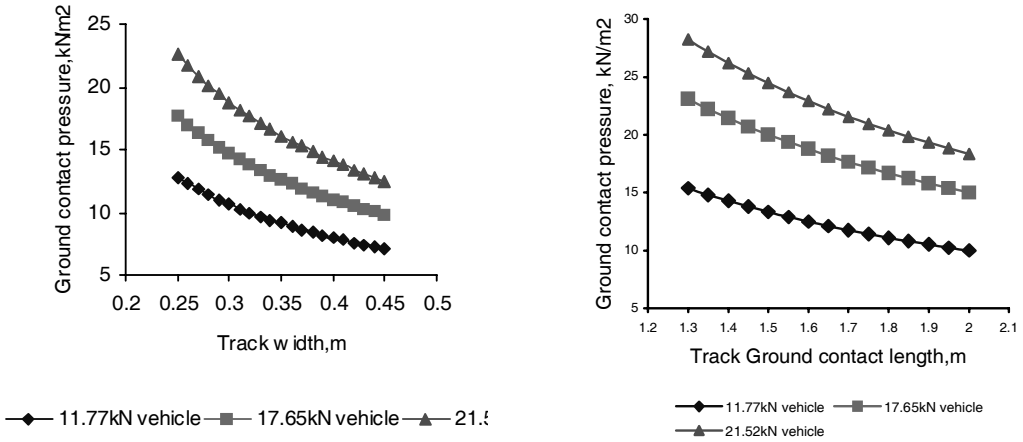

Fig. 5: Variation of ground pressure distribution with (a) variation of track width at constant track ground contact length of 200 cm and (b) variation of track ground contact length at constant track width of 30 cm.

Figs. 6 (a) and 6(b*)* show that the sinkage of the vehicle decreases with increasing track width and track ground contact length. If the track size of the vehicles is limited to 300x2000 mm^2, then the sinkage of the 11.77 kN, 17.65 kN, and 21.52 kN vehicles will be 61, 81.8, and 110 mm, respectively. From the field experiment, it was found that the surface mat thickness of the Sepang peat terrain was 100 mm, which will support the maximum load of the vehicle during static and dynamic as well. Therefore, if the vehicle

sinkage is more than 100 mm the vehicle will sink rather than traverse. If the vehicle total weight is considered to 19.62 kN and the track ground contact area to 300x2000 mm^2, the vehicle will traverse on the peat terrain with sinkage of 90 mm or 10 % less than the Sepang peat terrain surface mat thickness and exit ground pressure of 16 kN/m^2 or 6 % less than the worst condition Sepang peat terrain bearing capacity. Based on the 19.62 kN vehicle sinkage and ground contact pressure, it may be conclude that the vehicle will not in risk to traverse on peat terrain if the vehicle used the track ground contact area of 300x2000 mm^2.

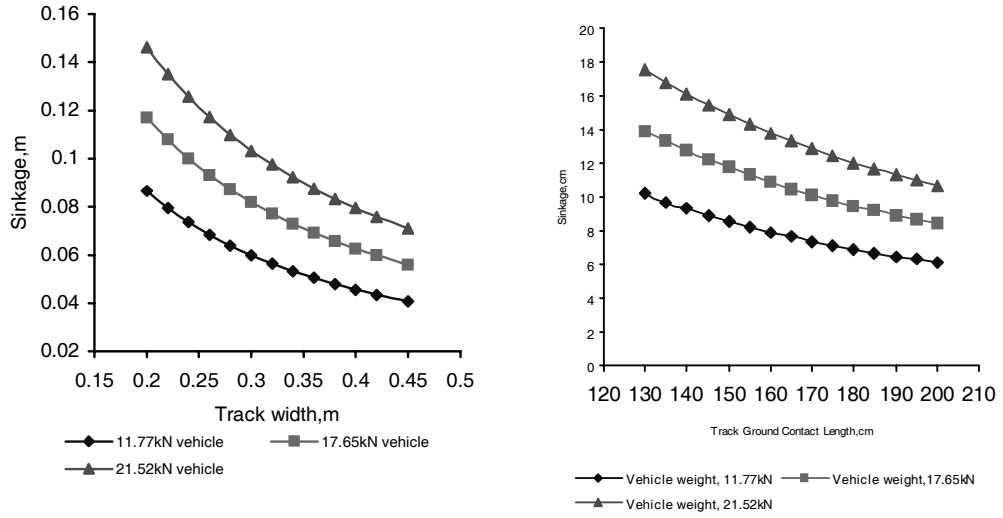

Fig. 6: Variation of vehicle sinkage with (a) variation of track width at constant track ground contact length of 200 cm and (b) variation of track ground contact length at constant track width of 30 cm.

Therefore, the best choice is to select a vehicle track ground contact area of 300x2000 mm^2 for the vehicle to produce an effective tractive performance.

The conclusion is further supported by the relation between the track size and motion resistance with keeping option either track width or track ground contact length could increase to adjust the track ground contact area for getting the desired vehicle ground contact pressure. Figures 7(a) and 7(b) show that the motion resistance coefficient of the vehicle increases with increasing track width and decreases with increasing track ground contact length. Figure 7(a) shows that the motion resistance coefficient increased 18.12 % for 13.73 kN vehicle, 16.99 % for 17.65 kN vehicle and 24.12 % for 21.58 kN vehicle with increasing the track width from 0.2 to 0.4m when the track ground contact length considered to keep in constant at 2.0m. Whereas, Fig. 7(b) shows that the vehicle motion resistance coefficient of the vehicle decreased 21.09 % for 13.73 kN vehicle, 24.07% for 17.65 kN vehicle and 24.5 % for 21.58 kN vehicle with increasing the track ground contact length from 1.3 to 2.2m when the track width considered to keep in constant at 0.3m. From the justification of vehicle motion resistance coefficient based on vehicle track width and track ground contact length, it could be noted that the vehicle track ground contact length should be considered to increase instead of increase the track width in order to get the vehicle lower ground contact pressure of 16 kN/m^2 on Sepang peat terrain.

Therefore, it was found that for a given overall dimension of 300x2000 mm^2 track system, the maximum motion resistance coefficient of the 19.62 kN vehicle is 5.4 %, which could be good enough for a track vehicle on soft terrain [7].

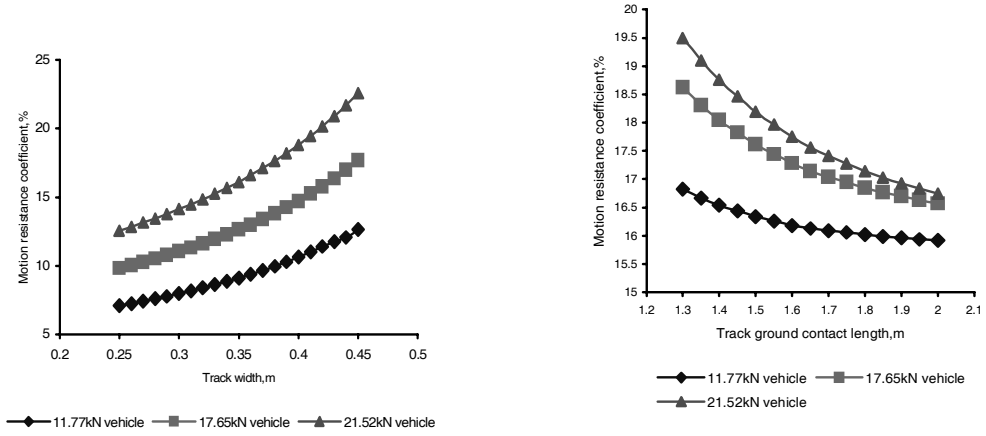

Fig. 7: Effect of track size on vehicle tractive performance (a) track width and (b) track ground contact

Based on Figs. 8(a) and 8(b), it could be pointed out that if the 19.62 kN vehicle track size is considered to be 300x2000 mm^2, the vehicle ground pressure exit on track-terrain interfaces is 16 kN/m^2 with sinkage of 90mm and motion resistance coefficient of 5.4%. Therefore, the 19.62 kN vehicle track system overall dimension can be optimized by selecting track width of 300 mm and ground contact length of 2000 mm.

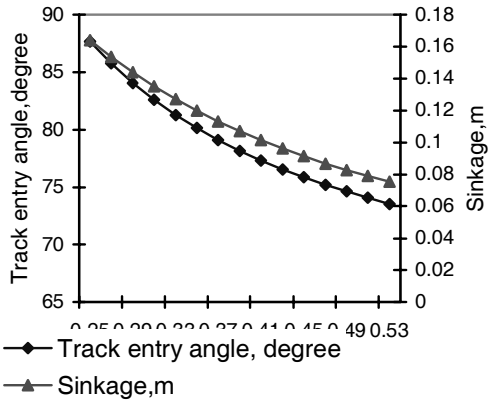

Fig. 8: Relationship between track entry angle, sinkage and idler diameter.

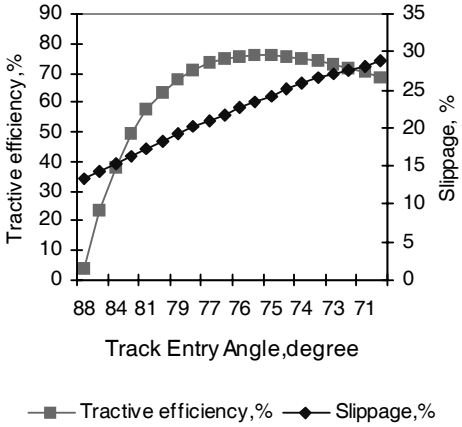

Fig. 9: Track entry angle, tractive performance and slippage.

4.2 Track Grouser Size

To fully utilize the shear strength of the peat surface mat for generating tractive effort, the use of grouser on tracks would be required. From the field experiment on Sepang, it was found that the shear strength of the peat surface mat is considerably higher than that

of the underlying peat deposit and that there is well defined shear-off point beyond which the resistance to shearing is significantly reduced. This would, however, considerably increase the risk of tearing off the surface mat unless the slip of the track is properly controlled. Thus, the use of aggressive grouser on vehicles for use in organic terrain does not appear to be desirable from traction as well as environmental viewpoints. The surface mat thickness of Sepang peat terrain was found to be about 0.1m. In order to fully utilize the shear strength of the surface mat and to increase the traffic ability of the terrain the grouser height of the track is considered to be 0.06 m.

4.3 Sprocket location and Size

The location of drive sprocket has a noticeable effect on the vehicle tractive performance. Wong et al. [6] (1986) reported that in forward motion, the top run of the track is subjected to higher tension when the sprocket is located at the front than when the sprocket is located at the rear. Thus, with a front sprocket drive, a larger proportion of the track is subjected to higher tension and the overall elongation and internal losses of the track will be higher than with a rear sprocket drive. With higher elongation, more track length is available for deflection and the track segments between road-wheels take fewer loads and the vibration of the track increase, which will cause the fluctuation of the track. Consequently, the sinkage and motion resistance will be higher and the mobility of the vehicle will be affected severely on the unprepared peat terrain. Therefore, the sprocket could be considered to locate at the rear part of the track system configuration in order to distribute the vehicle normal pressure to the track-terrain interfaces uniformly. The center point of the sprocket is considered the (0,0) coordinate system of the vehicle.

Generally, it could be mentioned that the sprocket is the most important component of the vehicle track system, which propels the vehicle with sufficient torque, control the vehicle speed fluctuation and maintain the vehicle tractive performance. Therefore, the size of the sprocket can be determined from the relationship between the relationship between the sprocket torque, vehicle speed fluctuation, and vehicle turning radius. From the simulation result, it was found that the ratio of the sprocket diameter to track pitch have significant effect on the vehicle tractive performance. Therefore, the ratio of the sprocket pitch diameter to track pitch should be a value which will stand to meet the field requirement.

Further support to optimize the sprocket size of the vehicle track system, the following equation on vehicle speed fluctuation can be considered. For the relation of vehicle speed fluctuation and the ratio of the vehicle sprocket pitch diameter to tract pitch the following mathematical model of Wong [7]can be used:

$$\delta = 1 - \sqrt{\left[1 - \left(\frac{1}{D_{prs}/T_p}\right)^2\right]} \qquad (13)$$

where δ is the speed fluctuation in percentage, D_{prs}/T_p is the sprocket pitch diameter to track pitch in proportion.

Using D_{prs}/T_p equals to 4.00, the computed value of δ is 3.17%. According to Wong [7], the industrial and agricultural track vehicle speed fluctuation should be in the range of 3.72 to 2.75%. Since the speed fluctuation of the vehicle was found of 3.17%, the ratio of the vehicle sprocket pitch diameter to track pitch can be optimized at 4.00. Consequently, the sprocket pitch diameter was optimized at 400mm by using the track pitch of 100mm.

4.4 Idler location and size

Idler is located at –2.0 m front of the track system. It was earlier reported that the surface mat thickness of Sepang peat terrain in the ranged of 100 to 250 mm which is considered the supporting platform of the vehicle. It could be noted that if the sinkage of any vehicle on the Sepang peat terrain is more than 100mm will cause the vehicle to bog down. Furthermore, from the simulation it was found that the track entry angle was significantly affect the vehicle front idler size and tractive performance. Therefore, from the relationship between the vehicle sinkage, track entry angle and idler diameter, the idler diameter can be identified. Figure 8 shows that the vehicle track entry angle at front idler and sinkage decreases with increasing vehicle front idler diameter. If the vehicle critical sinkage of the vehicle is considered to 100 mm, the corresponding front idler diameter and track entry angle were found 400 mm and 78°, respectively.

This conclusion can be further supported from the relationship between the track entry angle, slippage and vehicle tractive performance. Figure 9 shows that the relationship between the vehicle track entry angle, slippage, and tractive efficiency. At track entry angle 78°, the vehicle slippage and tractive efficiency were found 18% and 70.5%, respectively, which was found at sprocket pitch diameter of 400mm. Therefore, the front idler diameter 400mm can be optimized at 400mm for getting the tractive efficiency of the vehicle 70.5% and high productivity.

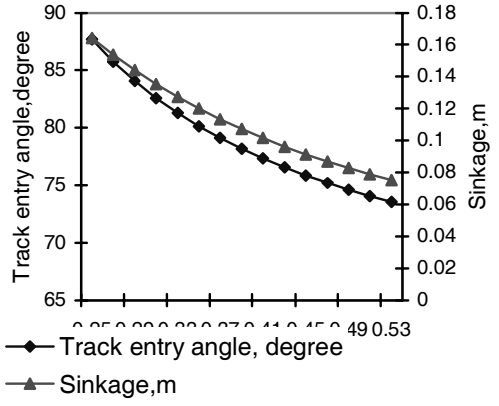

Fig. 8: Relationship between track entry angle, sinkage and idler diameter.

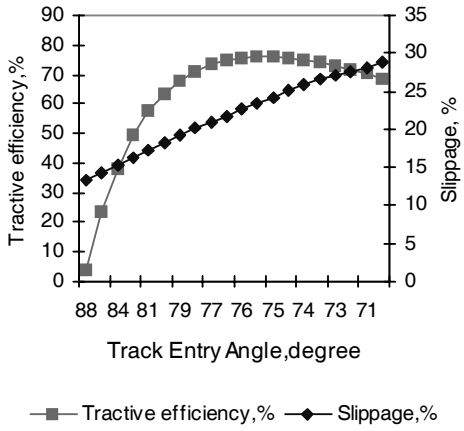

Fig. 9: Track entry angle, tractive performance and slippage.

4.5 Roadwheel diameter, Track pitch, and Number of Roadwheel

Wong [7] reported that the ratio of road wheel spacing to track pitch is a significant parameter that affects the tractive performance of tracked vehicle, particularly on soft

terrain. The decrease in the track motion resistance coefficient with the increase of the number of road wheels was primarily due to the reduction in the peak pressures and sinkage under the road wheels. The longer track pitch would lead to an improvement in tractive performance over soft terrain. But, it may cause a wider fluctuation in vehicle speed and higher associated vibration.

Consequently, a proper compromise between tractive performance and smoothness of operation must be struck. Road-wheel diameter can be predicted based on the following equation:

$$S_r = \frac{D_1}{2} + \frac{D_2}{2} + G \tag{14}$$

where, S_r is the road-wheel spacing in mm, D_1 is the first road-wheel diameter in mm, D_2 is the second road-wheel diameter in mm and G is the gap between consecutive road-wheel is assumed to be 5mm for avoiding the track deflection between the consecutive road-wheel.

In the track system all the road-wheel dimension ($D_1 = D_2$=------= D_7) are considered as equal size. If the roadwheel spacing equals to 225mm, the gap between two consecutive road-wheel on the track system equals to 5 mm, the computed value of road-wheel diameter equals to 220 mm.

Figure 10 shows that the vehicle drawbar pull increases with increasing the ratio road-wheel spacing to track pitch and tractive efficiency increases with increasing the ratio of road-wheel spacing to track pitch until 2.1 and then decreases with further increasing of the ratio of road-wheel spacing to track pitch. If the ratio of road-wheel spacing to track pitch is considered to be 2.25, the tractive efficiency of the vehicle is found 70.5%. Whereas, the tractive efficiency of the vehicle is found 70.5% for the optimum sprocket pitch diameter of 400 mm and idler diameters of 400 mm. Therefore, the ratio of road-wheel spacing to track pitch should be 2.25 if the optimum sprocket pitch diameter and idler diameters each is limited to 400 mm. By using S_r/T_p equals to 2.25 and S_r equals to 225mm, the computed value of T_p equals to 100 mm.

The number of road-wheels can be computed based on Fig. 2 by the following equation [5]:

$$n_r = \frac{\left(L - \left((D_{rs} + D_{fi})/2\right)\right)}{\left(D_r + G\right)} \tag{15}$$

where, L is the total ground contact length in mm, D_{rs} is the outside diameter of the sprocket in mm , D_{fi} and D_r are the diameter of the front idler and road-wheel in mm and n_r is the number of road-wheel. The outside diameter of the sprocket (i.e, $D_{rs} = D_{prs} + H/2$) is considered to 460mm based on the grouser height.

By using L equals to 200 mm, D_{rs} equals to 460 mm, D_{fi} equals to 400 mm, D_r equals to 220 mm, G equals to 5mm, the computed value of n_r is 7. Therefore, total number of road-wheel seven with diameter of 220 mm on the 19.62 kN vehicle track system would

significantly reduce vehicle vibration during traversing on the unprepared peat terrain by making zero deflection of the track between two consecutive road-wheel.

4.6 Center of Gravity Location

Center of gravity of a tracked vehicle is a most important design parameter for getting the high tractive performance. Figure 12 shows that the tractive efficiency of the vehicle increases steeply with increasing the slippage of the vehicle until a certain value and then start to decrease with increasing the slippage of the vehicle. The vehicle under consideration with total weight 19.62 kN including payload of 5.89 kN is traversing on a zero slope terrain with traveling speed of 10 km/hr. Figure 11 shows the maximum tractive efficiency of 79.8% at 11% slippage for the vehicle with center of gravity located at 300 mm rearward from the mid-point of the track ground contact length and 70.5% at 12% slippage for the vehicle with center of gravity located at the mid-point of the track ground contact length.

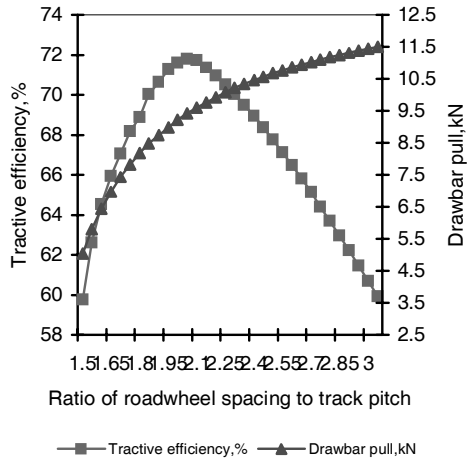

Fig.10: Relationship between tractive efficiency, drawbar pull and the ratio of the road-wheel spacing to track pitch

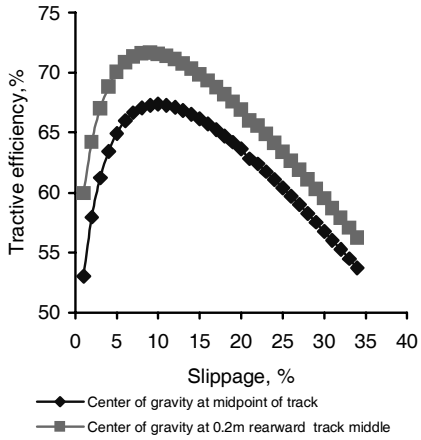

Fig. 11: Relationship between tractive efficiency and slippage.

From the comparison of the vehicle based on the location of center of gravity, it is found that the tractive efficiency of the vehicle with center of gravity is located at 200 mm rearward from the mid point of the track ground contact length is 13.2% higher than the tractive efficiency of the vehicle with the center of gravity is located at the mid-point of the track ground contact length. The variation of tractive efficiency is found between the vehicle with the locations of center of gravity due to the difference of external motion resistance. It could be pointed out that the vehicle with location of center of gravity at 200mm rearward from the mid point of the track ground contact length reveals lower sinkage at the frontal part of the track ground contact part causes the lower external motion resistance and the vehicle consume lower engine power for developing effective tractive effort in order to traverse the vehicle easily on the low bearing capacity peat terrain. Whereas, the vehicle with location of center of gravity at the midpoint of the track ground contact length reveals the equal sinkage to all over the ground contact part causes

the higher external motion resistance and vehicle consume maximum engine power for developing the required tractive effort in order to traverse the vehicle on the low bearing capacity peat terrain. Therefore, the vehicle center of gravity location of 300mm rearward from the mid-point of the track ground contact length could be optimized the center of gravity location for the vehicle.

The basic design parameters of the vehicle found from the simulation study are shown in Table 7

Table 7. Basic design parameters of the special segmented rubber tracked vehicle

Vehicle Parameters		
Total weight including 9.81kN payload, kN	W	19.62
Vehicle traveling speed, km/hr	v_t	10
Center of gravity, x coordinate, m	x_{cg}	-0.80
Centre of gravity, y coordinate,m	y_{cg}	0.45
Sprocket pitch diameter , m	D_{rs}	0.40
Idler diameter, m	D_{fi}	0.40
Idler center, x coordinate, m	x_{cfi}	-2.0
Idler center, y coordinate, m	y_{cfi}	0
Number of road-wheels (each side)	n	7
Road-wheel diameter, m	D_r	0.22
Road-wheel spacing, m	S_r	0.225
Number of supporting rollers (each side)	n_s	3
Supporting rollers diameter, m	D_s	0.20
Track Parameters		
Track total length (each side), m	L_c	5.90
Track pitch, m	T_p	0.10
Track width, m	B	0.30
Track ground contact length, m	L	2.00
Road-wheel spacing to track pitch	S_r/T_p	2.25
Vehicle speed fluctuation, percentage	δ	3.17
Grouser height, m	H	0.06

Note: Coordinates origin is at the center of the sprocket. Positive x and y coordinates are to the rear and top, respectively.

5. CONCLUSION

The following conclusions were made based on the analysis of this paper:

Based on the results of mechanical properties of peat in the area studied, the mean values for moisture content of 79.58%, bulk density of 1.53kN/m^3, cohesiveness of 1.36kN/m^3, internal friction angle of 26.22°, shear deformation modulus of 11.2mm, surface mat stiffness of 13.6kN/m^3, and underlying peat stiffness of 171.54kN/m^3.

Based on the results of detailed study on vehicle parameters, an optimized track system configuration for the 19.62kN vehicle has seven roadwheels with diameter of 0.24m, a track pitch of 0.1m, a ratio of the initial track tension to vehicle weight of 12%, a location of center of gravity at 30cm rearward of the mid-point of the track ground contact length ensure the vehicle to develop the maximum tractive efficiency of 74% during traversing at 10km/hr on the specified peat terrain.

Based on the simulation study, it was found that the track pitch, number of road wheels, and location of centre of gravity have noticeable effects on the tractive performance of the vehicle. The maximum tractive efficiency of the vehicle is in the range of 74 to 72 % and 50 to 48% with the slip range of 9 to12% when the vehicle traveled at 10km/hr without payload and with payload, respectively. Furthemore, the tractive efficiency of the vehicle with center of gravity located at 300mm rearward of the mid-point of track ground contact length are 10% higher than the vehicle center of gravity located at the mid-point of track ground contact length.

ACKNOWLEDGEMENT

This research project is classified under RM7 IRPA Project No. 01-02-04-0135. The authors are very grateful to the Ministry of Science, Technology and The Environment of Malaysia for granting the financial assistance.

REFERENCE

[1] ASAE, *Agricultural Engineers Yearbook of Standards*, American Society of Agricultural Engineers, Michigan (1996).

[2] Ataur, R, Azmi, Y, Zohadie, M, Desa, A, Wan, I, and Kheiralla, A. (2004) Mechanical Properties in Relation to Vehicle Mobility of Sepang Peat Terrain in Malaysia. Journal of Terramechanics, Elsevier Publisher: 41(1), pp24-45.

[3] Ataur, R., Azmi, Y., Zohadie, M., Ahmad, D and Ishak, W. (2005a). Simulated Steerability Of A Segmented Rubber Tracked Vehicle During Turning On Sepang Peat Terrain in Malaysia. *Int. J. of Heavy Vehicle Systems* (IJHVS), Inderscience Publisher, UK: Vol.12, No. 2, pp. 139-168.

[4] Ataur, R., Azmi, Y., Zohadie, M., Ahmad, D and Ishak, W . (2005b). Design and Development of a Segmented Rubber Tracked Vehicle for Sepang Peat Terrain in Malaysia. *Int. J. of Heavy Vehicle Systems* (IJHVS), Inderscience Publisher, UK: Vol.12 No.3.

[5] Ataur, R., Azmi, Y., Zohadie, M. Ishak, W and Ahmad, D. (2005c). Design Parameters Optimization Simulation of a Segmented Rubber Tracked Vehicle for

Sepang Peat in Malaysia. American Journal of Applied Science, Science Publications, New York, USA: Vol.2(3), pp.655-671.

[6] Ooi,H.S.(1986) Performance of Modified Kubota Carrier RC20P and Porter P6-121 on peat soil. MARDI Report no.110.

[7] Wong, J.Y. (1998) Optimization of design parameters of rigid-link track systems using an advanced computer aided method. Proc. Instn. Mech. Engrs, 208(D), pp153-167.

Biographies of all authors are missing